Chapter 5: Calibration and Testing

5.1 Experimental Setup

Figure 5.1 shows the schematic of the sensors used in the testing and calibration of the magnetometer system. Since the phase variation of each sensor on application of external magnetic field depends on a variety of external factors, it is essential to calibrate each axis independently. The voltage output of each sensor primarily depends on its operating point, fringe visibility and the strain induced in it due to bending of the fiber.

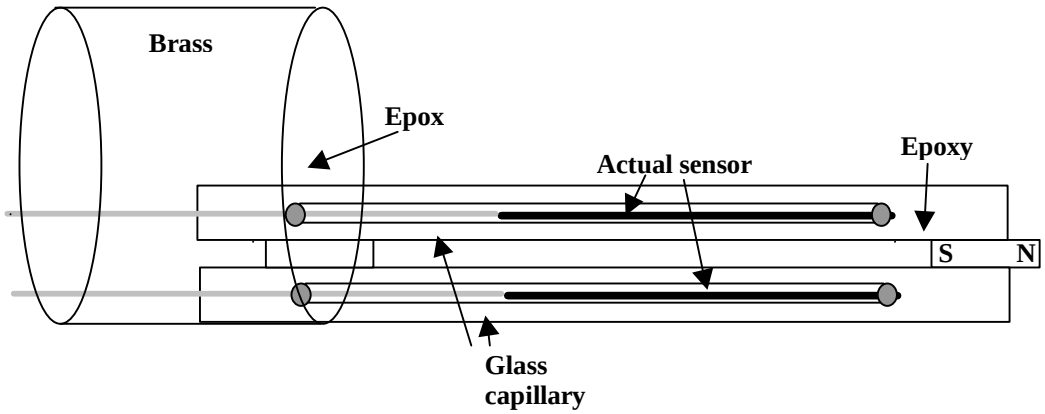

Figure. 5.1 Schematic of a single axis sensor assembly.

As shown in the figure, each individual sensor consists of an EFPI with the sensing fiber replaced by a magnetostrictive wire about 125 μm in diameter. The wire is field-annealed and polished at an angle to increase the fringe visibility of the sensor output. Both the reference fiber and the sensing wire are enclosed in a Boro-silicate glass tube with an ID of about 150 μm. The tube is sealed at both ends using commercial grade epoxy. Each sensor is then sealed inside a glass capillary tube. Two such sensors, which are in quadrature, are then glued together along with a single permanent magnet for DC bias, using epoxy. The quadrature phase shifted sensor

pair is then attached to the inner surface of a small length of brass tube. This reduces the bending-induced strain on the sensors as well as facilitates the insertion of the assembly into the Aluminum sensor head.

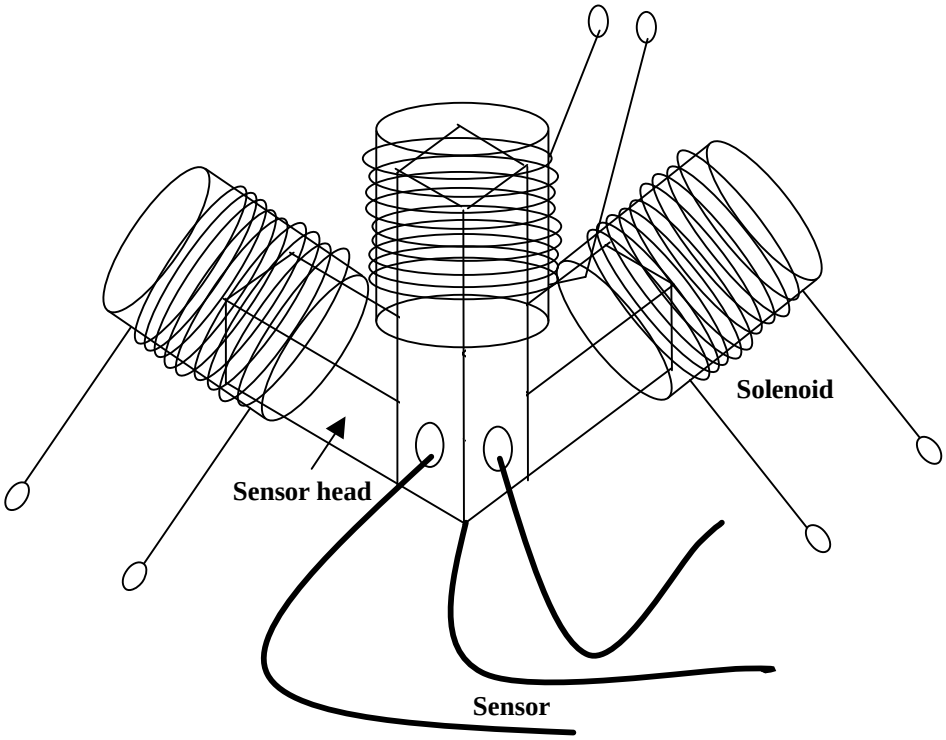

Figure 5.2 Experimental setup.

Figure 5.2 shows the overall experimental setup. The quadrature phase shifted, DC field biased sensor pairs are inserted along the three axes of the Aluminum sensor head with minimal strain. Each arm of the sensor head is placed in a solenoid capable of producing the necessary calibration flux density. Once the setup is complete, the assembly is allowed to stabilize for some time. The first part of the experimental procedure deals with determining the magnetic field response of each of the individual sensors. In the second part, the microprocessor-based signal demodulation system calculates the overall signal for each axis. This is essentially the calibration procedure where the relation between the calculated output and the applied external magnetic field is determined. The signal demodulation system samples each sensor output at a

rate of 18 Hz. The digitized signal is then averaged over two seconds, normalized to the laser source variation and then used in further calculations. The following sections describe the calibration procedure and the obtained results in detail.

5.2 Calibration Procedure

In order to determine the magnetic field response of each sensor, the sensor pair under investigation was placed inside the calibration coil. The operating point of the sensor with respect to its peak to peak value was observed. This is one of the critical factors in obtaining the magnetic response as will be seen from the results. A DC magnetic field was then applied and varied in steps from – 40,000 nT to 40,000 nT. The voltage output of each sensor for the applied magnetic fields was observed and measured using an oscilloscope. The procedure was repeated one more time and a similar reading was obtained. The magnetic field response (low and high field) for each sensor was plotted. These results are presented in the next section.

Figure 5.3 shows the typical variation in an EFPI sensor output due to change in phase between the reference and sensing reflections. V_{ref} in the figure denotes the initial operating point the sensor. As can be seen from the figure, the movement of the operating point along the slope depends on the overall applied magnetic field and can thus be used to measure the direction of the applied field.

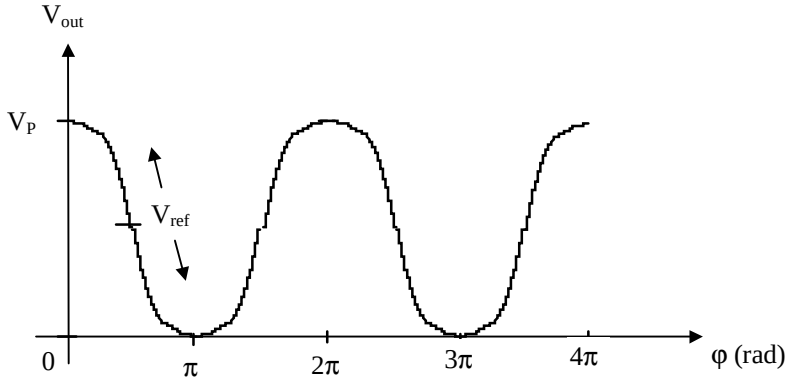

Figure 5.3 Initial operating point of the sensor.

If the direction of the external applied magnetic field is opposite to that of the biasing field, the overall magnetic field applied to the sensor decreases and so does the length of the metglas wire. Thus the phase difference between the first and second reflection increases. If the sensor operates at the point shown in Figure 5.3, the output voltage falls below the reference voltage. In case the direction is same as that of the biasing field, the output voltage goes above the reference voltage. Thus the direction of the applied magnetic field can be easily determined. From the results obtained in the first part of the experiment the sensors which show the above response are identified. These are generally the sensors operating around the middle of the fringe output. One sensor from each pair is thus used to determine the direction of the external applied magnetic field along that particular axis. This information was used to modify the application program driving the microprocessor-based signal demodulation system. In the second part of the experiment, the signal demodulation system displayed the overall output corresponding to each axis after performing various operations on individual sensor outputs in each pair. The magnetic field was again varied from – 40,000 nT to 40,000 nT in steps and the displayed output was recorded. The calibration curve (displayed output vs. external applied magnetic field) was plotted for each sensor pair. These results are also presented in the following section. Figure 5.4 shows the magnetostriction response of the sensor material. As can be seen from the figure, the output of the sensor will be non-linear if the sensor is not biased in the linear range of operation.

5.3 Experimental Results

The plots showing the results of the experiments described above are presented below. Figures 5.5 (a) and (b) show the low and high field response of sensor 3 respectively. As can be seen from the figures, the low field response is more linear than the high field response. This discrepancy is because although the sensor operates in the linear range of the fringe at lower field strengths, at higher fields the region of operation is no longer linear. This effect is more clearly visible in some of the plots presented later.

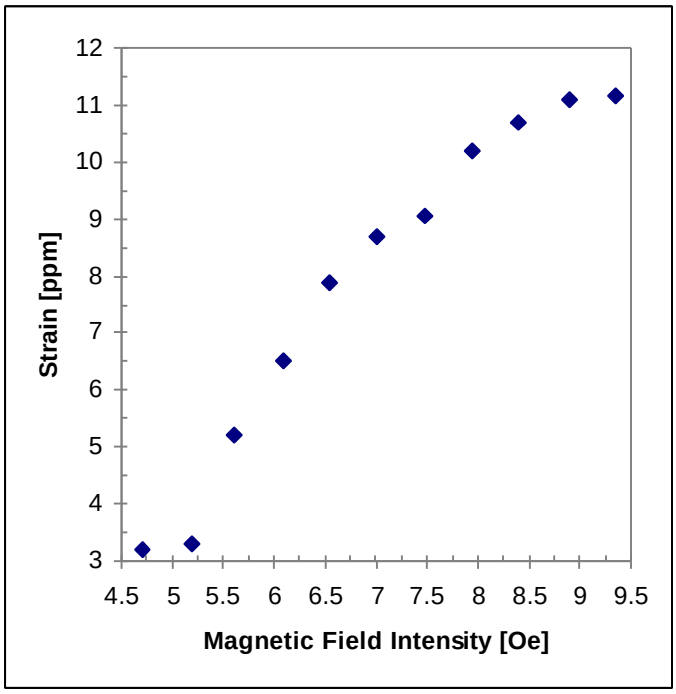

Figure 5.4 Magnetostrictive response of metglas material.

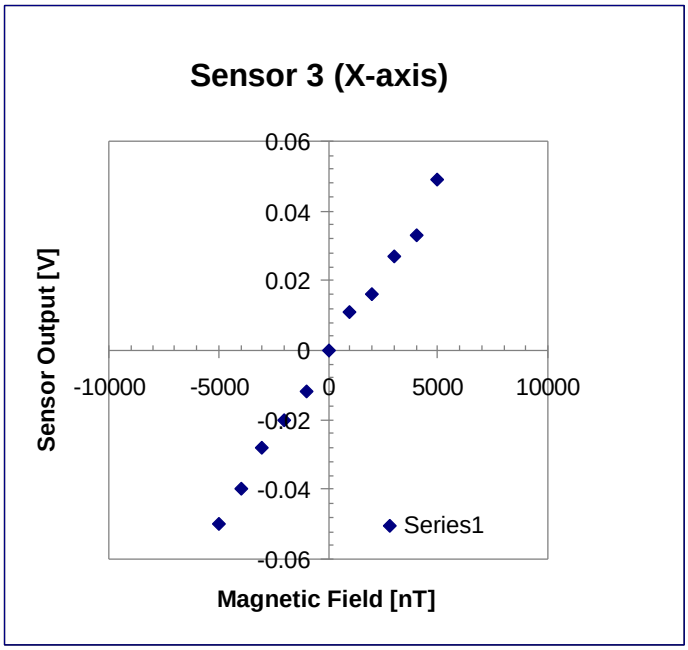

Figure 5.5 (a) Low field response of sensor 3 (X-axis).

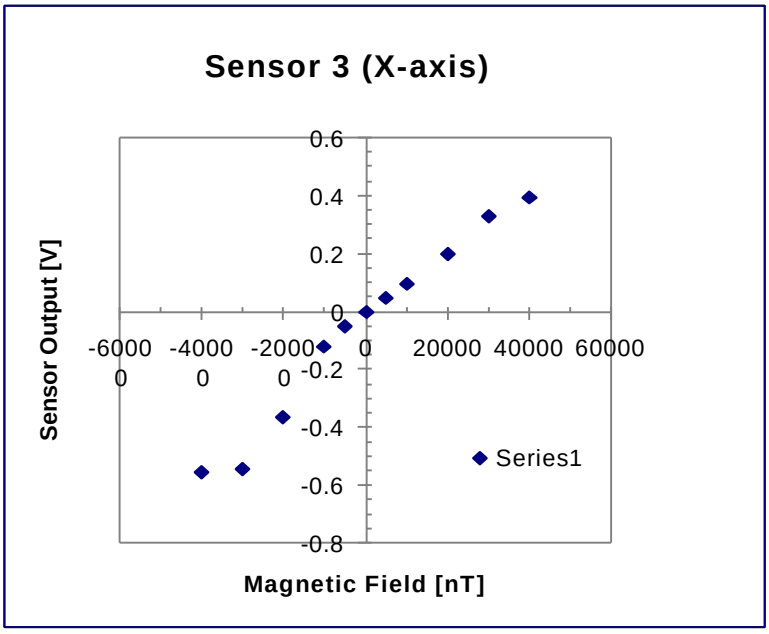

Figure 5.5 (b) High field response of sensor 3 (X-axis).

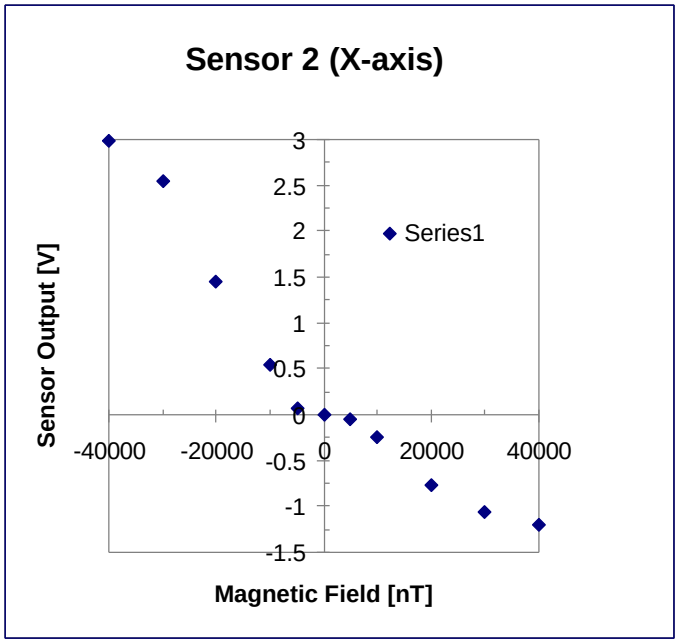

Figure 5.6 Field response of sensor 2 (X-axis).

As can be seen in Figure 5.6, sensor 2 does not show a good low field response. Since the initial operating point of this sensor is 90^0 out of phase with that of sensor 3, it operates either near the top or the bottom of the fringe and hence shows extremely low sensitivity. The plot also indicates that the operating point is not exactly at the bottom or top. If this were the case, the output voltage variation on application of positive and negative magnetic fields would be in the same direction.

Figs. 5.7 (a) and (b) show the magnetic field response of sensor 4. As can be seen from the figures, the response is exactly opposite to that shown by sensor 3. The direction of voltage variation depends not only on the operating point along the fringe but also on the slope of operation. Sensor 4, though operating near the center (as can be seen from the linear low-field response), operates on the other side of the fringe (similar to sensor 2) and hence shows an output variation exactly opposite of that shown by sensor 3.

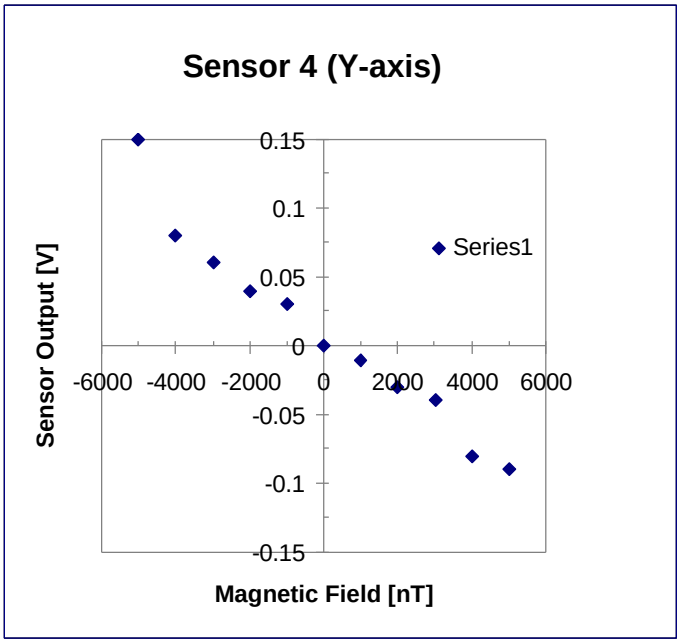

Figure 5.7 (a) Low field response of sensor 4 (Y-axis).

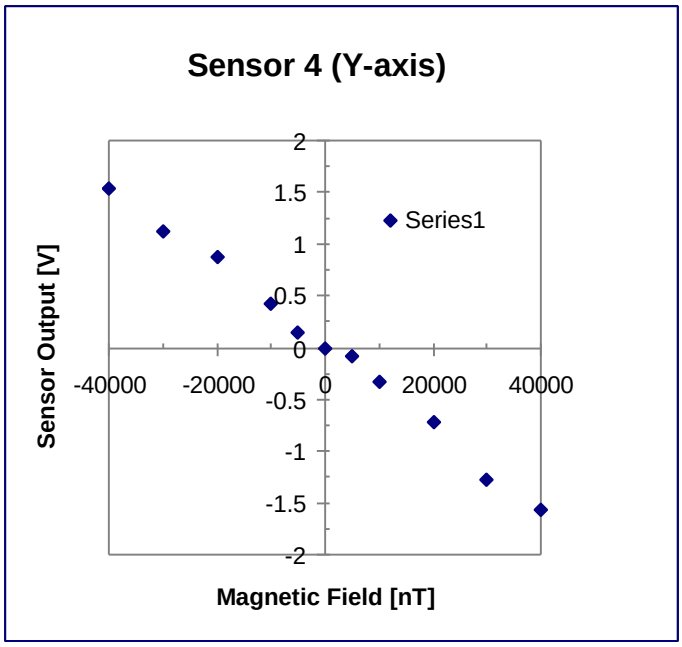

Figure 5.7 (b) High field response of sensor 4 (Y-axis).

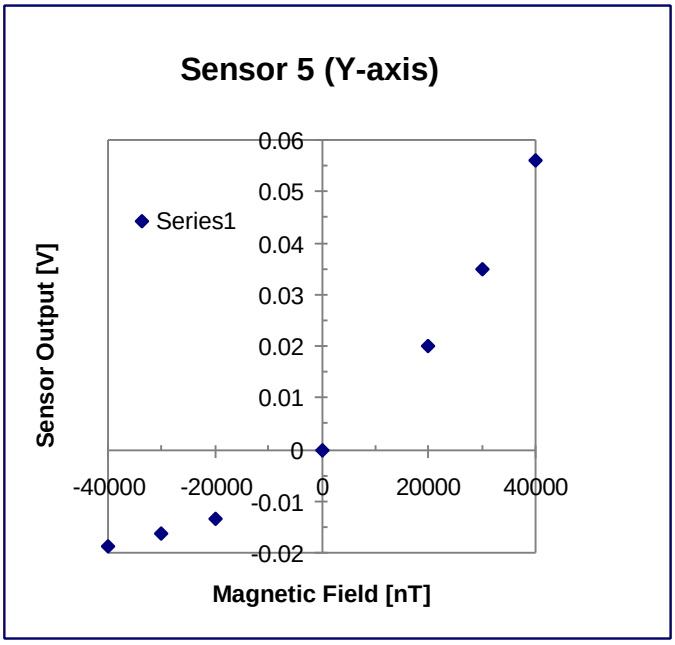

Figure 5.8 Field response of sensor 5 (Y-axis).

As can be seen in Figure 5.8, sensor 5 exhibits a response similar to that shown by sensor 2. It operates either near the bottom or the top of the fringe and hence shows extremely low sensitivity. Like sensor 2, the operating point is not exactly at the peak. However the slope of operation is similar to that of sensor 3.

Figs. 5.9 (a) and (b), and Figs. 5.10 (a) and (b) show the low and high field response of sensors 6 and 7 respectively. As can be seen from the figures, both the sensors show visibly non-linear response even for low fields. The sensors, though in quadrature with each other, operate near the top and bottom of the fringe and thus in the non-linear region of operation. Hence the non-linear response.

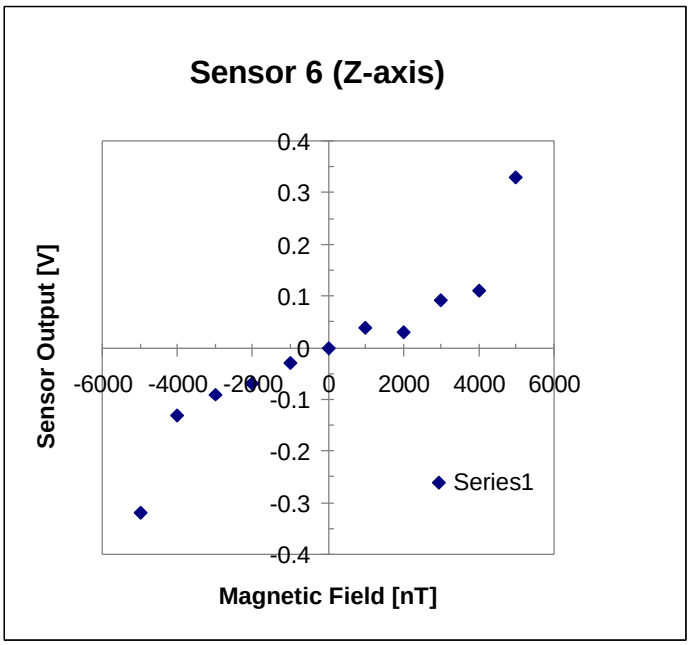

Figure 5.9 (a) Low field response of sensor 6 (Z-axis).

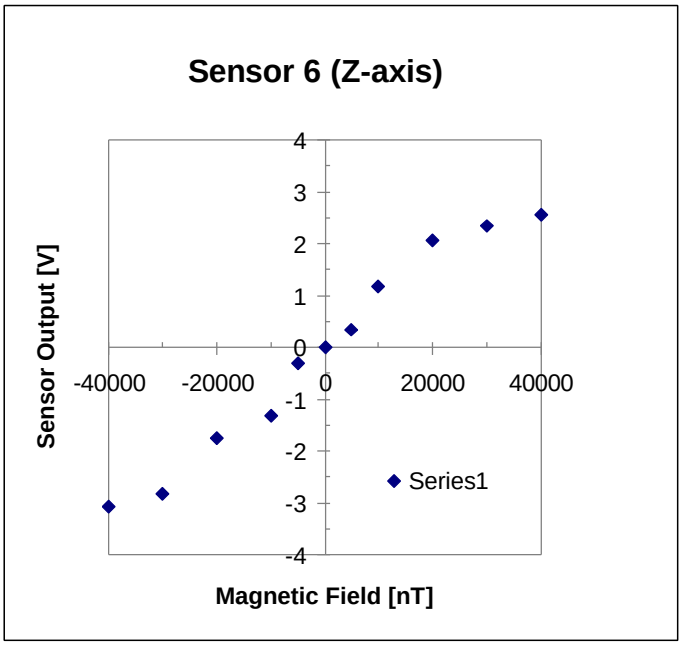

Figure 5.9 (b) High field response of sensor 6 (Z-axis).

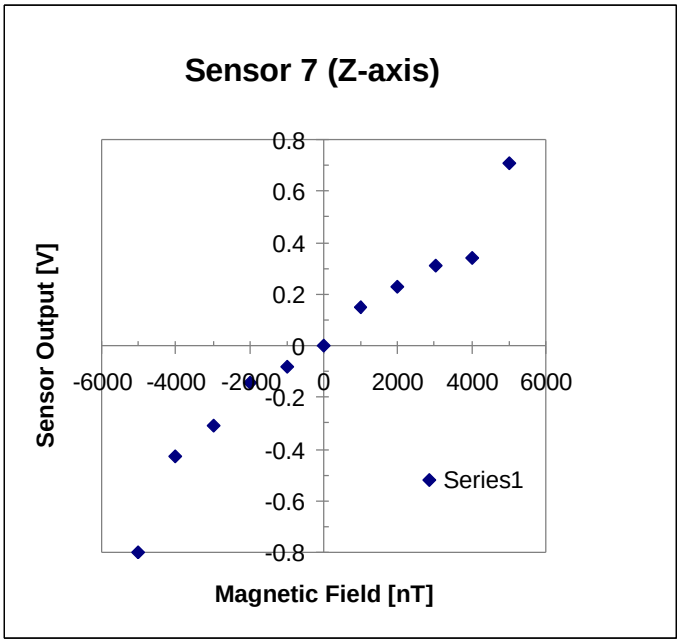

Figure 5.10 (a) Low field response of sensor 7 (Z-axis).

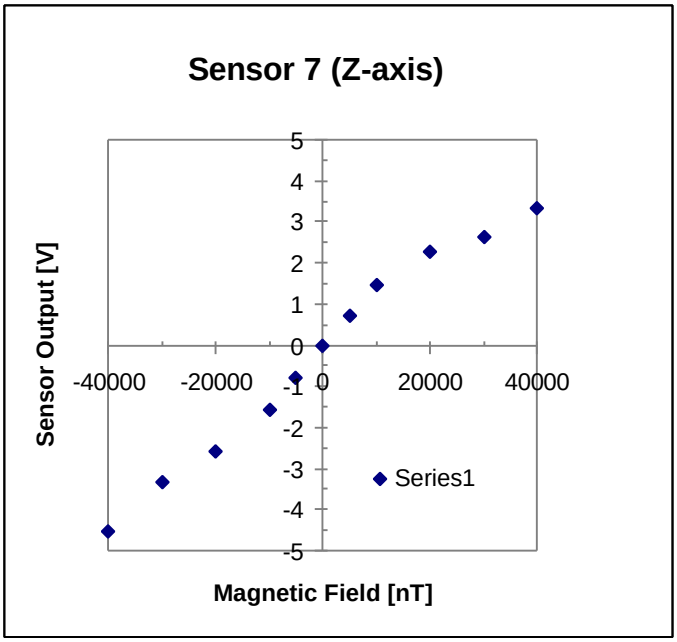

Figure 5.10 (b) High field response of sensor 7 (Z-axis).

Figures 5.11, 5.12 and 5.13 show the calibration curves for the X, Y and Z axes of the magnetometer system. The figures show the output calculated by the signal demodulation system, plotted against the applied external magnetic field. All the calibration curves exhibit a certain level of non-linearity which can be attributed to the non-uniform response of the individual sensors to the same external applied field. That is, the quadrature phase relation between the two sensors of a pair is not maintained over the entire range of operation. The implications of the above results and the conclusions drawn, are presented in the concluding chapter of the thesis.

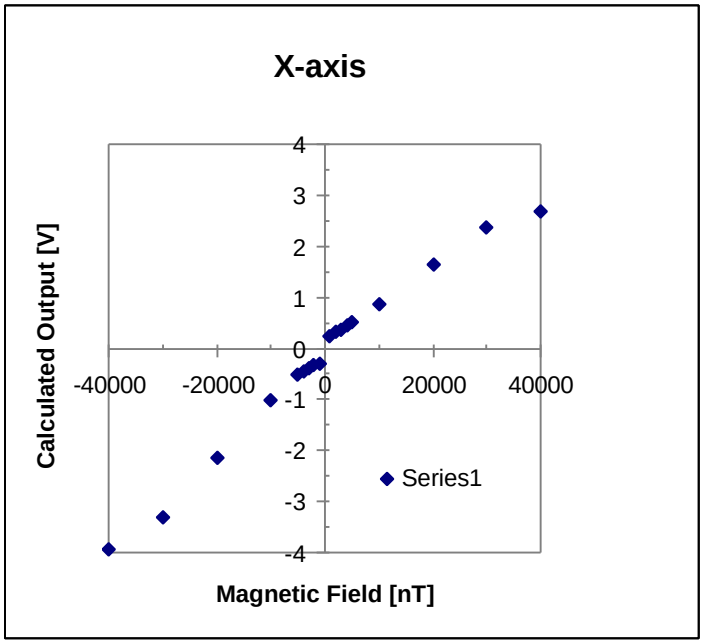

Figure 5.11 Calibration curve for X-axis.

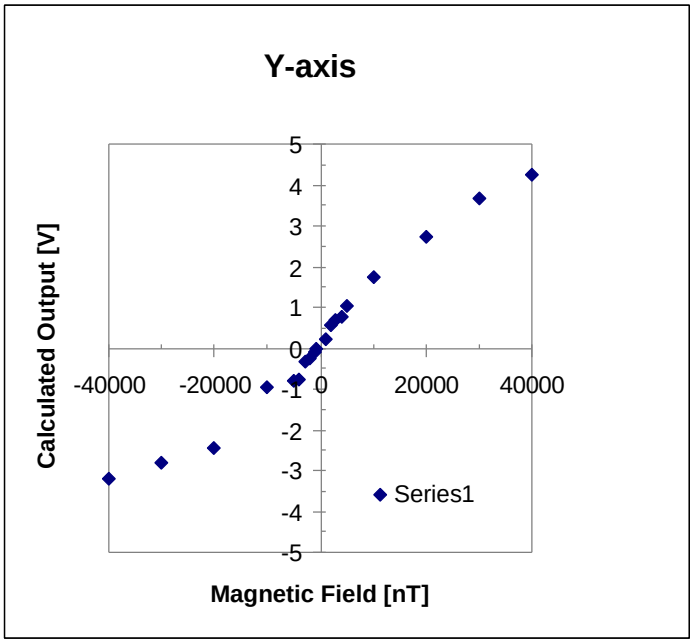

Figure 5.12 Calibration curve for Y-axis.

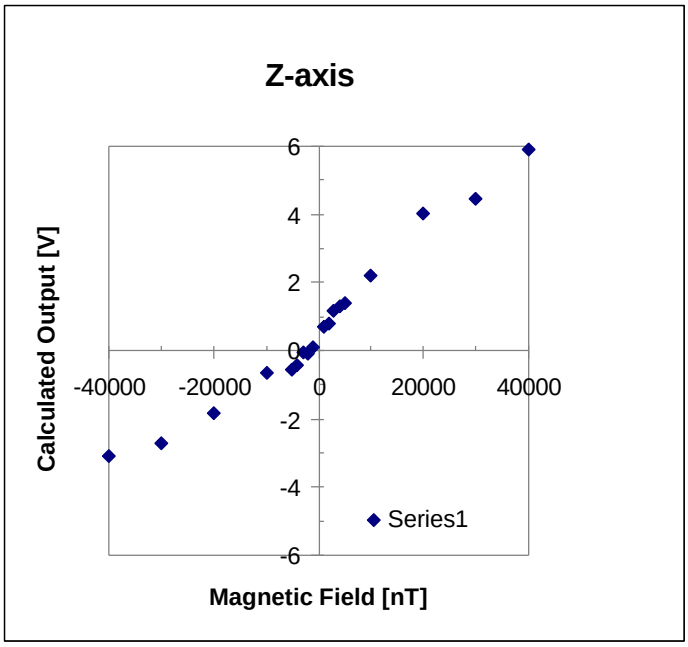

Figure 5.13 Calibration curve for Z-axis.

Figure 5.14 Experimental arrangement of magnetometer system.

Figure 5.15 Electronic signal processing system box.

Figure 5.16 Calibration setup.

Figure 5.17 Complete experimental setup.